PREPARED FOR THE U.S. DEPARTMENT OF ENERGY,
UNDER CONTRACT DE-AC02-76CH03073

PPPL-3516
UC-70

PPPL-3516

High Harmonic Fast Wave Heating Experiments on NSTX

by

J.R. Wilson, R. Bell, M. Bitter, P. Bonoli, M. Carter, D. Gates,
J.C. Hosea, B. LeBlanc, R. Majeski, T.K. Mau, J. Menard, D Mueller,
S. Paul, C.K. Phillips, R. Pinsker, A. Rosenberg, P. Ryan,
S.A. Sabbagh, D. Stutman, D. Swain, Y. Takase, J. Wilgen

November 2000

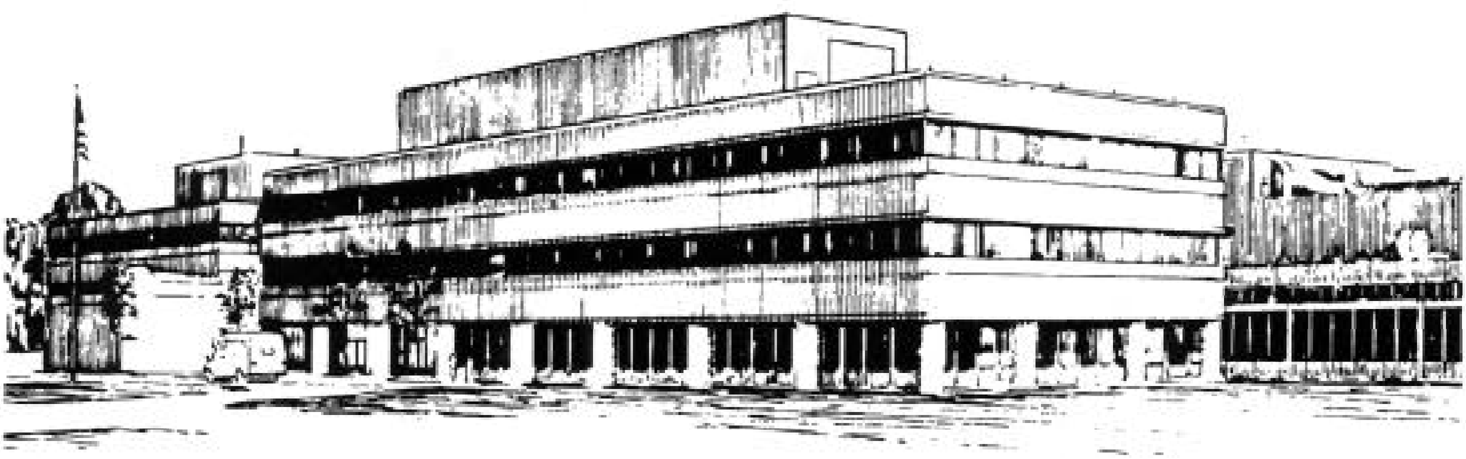

PRINCETON PLASMA PHYSICS LABORATORY
PRINCETON UNIVERSITY, PRINCETON, NEW JERSEY

High Harmonic Fast Wave Heating Experiments on NSTX

J. R. Wilson 1), R. Bell 1), M. Bitter 1), P. Bonoli 2), M. Carter 3), D. Gates 1),
J. C. Hosea 1), B. LeBlanc 1), R. Majeski 1), T. K. Mau 4), J. Menard 1), D Mueller 1),
S. Paul 1), C. K. Phillips 1), R. Pinsker 5), A. Rosenberg 1), P. Ryan 3), S. A. Sabbagh 6),
D. Stutman 7), D. Swain 3), Y. Takase 8), J. Wilgen 3)

1) Princeton Plasma Physics Laboratory, Princeton NJ, USA
2) Massachusetts Institute of Technology, Cambridge MA, USA
3) Oak Ridge National Laboratory, Oak Ridge TN, USA
4) University of California at San Diego, San Diego CA, USA
5) General Atomics, San Diego CA, USA
6) Columbia University, New York NY, USA
7) Johns Hopkins University, Baltimore MD, USA
8) University of Tokyo, Tokyo, Japan

e-mail contact of main author: jrwilson@pppl.gov

Abstract. A radio frequency (rf) system has been installed on the National Spherical Torus Experiment (NSTX) with the aim of heating the plasma and driving plasma current. The system consists of six rf transmitters, a twelve element antenna and associated transmission line components to distribute and couple the power from the transmitters to the antenna elements in a fashion to allow control of the antenna toroidal wavenumber spectrum. To date, power levels up to 3.85 MW have been applied to the NSTX plasmas. The frequency and spectrum of the rf waves has been selected to heat electrons via Landau damping and transit time magnetic pumping. The electron temperature has been observed to increase from 400 to 900 eV with little change in plasma density resulting in a plasma stored energy of 59 kJ and a toroidal beta, β_T , =10% and β_n = 2.7.

1. Introduction

The NSTX device is a small aspect ratio toroidal plasma device designed to operate at high beta [1]. A major research goal of the NSTX program is to demonstrate that such devices are capable of sustained plasma operation with a small or no ohmic heating transformer. One attractive feature of ST devices is the large bootstrap current achievable. This means that during the steady flattop portion of the discharge only a small fraction, ~ 30%, of the current needs to be driven by external means. However, an external method of ramping up the plasma current and beta would still be required to reach the flattop conditions.

It has been proposed [2] that high harmonic fast waves (HHFW) can be utilized to heat electrons and drive plasma current to satisfy the above requirements. The naturally high beta in an ST leads to strong absorption of the rf waves by the electrons even at modest plasma parameters. The low toroidal field value of NSTX also allows the use of conventional ICRF frequencies and equipment. In this case we have utilized the TFTR ICRF transmitters and transmission line components operating at a frequency of 30 MHz.

2. Description of HHFW System

The HHFW system is comprised of six rf transmitters operating at a frequency of 30 MHz, a transmission system comprised of standard coaxial transmission lines each having an adjustable tuning stub and phase shifter, a decoupling and power splitting network, and a twelve element antenna array (FIG. 1) [3].

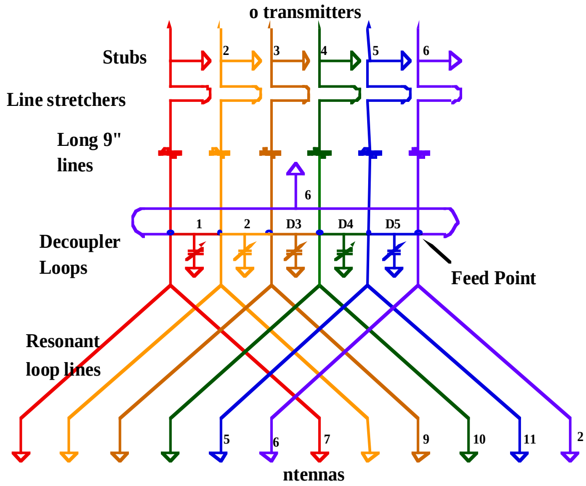

Figure 1. Schematic of the NSTX HHFW System

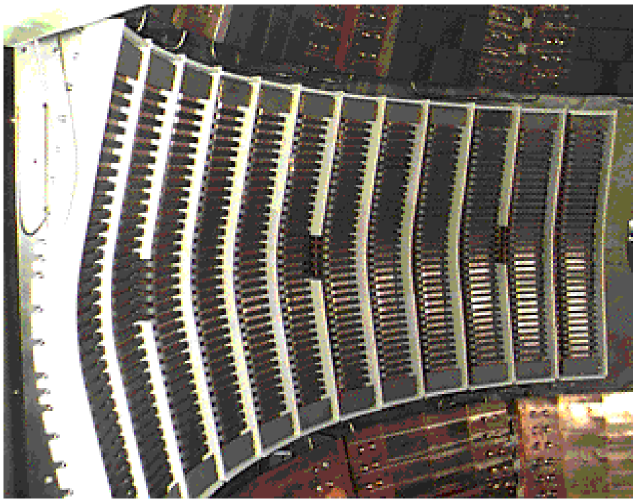

Figure 2 HHFW antenna array inside NSTX

Each transmitter is rated for 1.0 MW for 5 s into a load with a VSWR of 3:1. The phase of each transmitter can be electronically varied to control the antenna spectrum. Active feedback control of the antenna phasing will be implemented in the future.

The decoupling and power splitting network consists of resonant loops of six-inch coaxial line connecting the i^{th} and $6+i^{th}$ elements of the antenna [4]. The total length of each of the resonant circuit is 2 λ including the antenna elements. The feedpoints are located 3/4 λ from one end of each resonant circuit and the six decoupling loops are also attached at these point. These decoupling loops, which connect the neighboring feedpoints, consist of an appropriate length of 93 ohm transmission line with a parallel reactive element at the midpoint of the loops. For five of these loops the required element is a capacitance which is provided by a commercially available vacuum variable capacitor. For the sixth element, which connects the end back to the beginning of the array, an inductive reactance is required. This reactance is provided by a length of shorted transmission line.

The antenna array is composed of twelve modules (FIG. 2). Each module is self contained and supported by the vacuum feedthrough and the vessel wall. Boron nitride insulating plates separate each antenna element and protect the top, bottom and ends of the array. The antenna elements are shorted at the bottom and fed at the top and are separated from the plasma by a single layer molybdenum Faraday shield.

3. Properties of the Decoupling Network

The purpose of the decoupling and power splitting network is to allow equal feedline powers to result in equal antenna element currents that have a selectable phase relationship to one another. The resonant loops connecting the i^{th} and $i+6^{th}$ antenna elements provide an even power division and a fixed phase relationship between these elements. In the absence of the decoupling loops, the mutual inductance between the antenna elements would only allow phases of 0^0 and 180^0 for the loops with equal antenna currents for equal feed powers. The decoupling loops provide a shunt coupling between the various feed circuits that can, in principle, exactly cancel the mutual coupling from the nearest neighbor antenna element.

The electrical properties of the six resonant antenna circuits can be completely described by the elements of the 6 by 6 S matrix. The elements, S_{ij}, of the matrix describe the magnitude and phase of the power that would appear at the j^{th} feedpoint if a unit power is injected at the i^{th} feedpoint. The presence of the decoupler reduces the magnitude of the first off diagonal elements, $S_{i,\, i\pm1}$, from 0.25 to 0.0023. The largest elements are then the next nearest neighbor, $S_{i,\, i\pm2}$, elements whose magnitude is 0.043

On NSTX a long, ~ 85 m, run of transmission line exists between the feedpoints and the tuning network. The tuning network transforms the circuit impedance to the characteristic impedance of the transmission line from the transmitters. If this transformation is exact the transmitters will see no reflected power. When we look at the S matrix for the antenna system on the input side of the tuning we observe a stronger coupling between the first, third and fifth lines and also the second, fourth and sixth. This coupling is strong enough in vacuum to require tuning the triplets iteratively. When operated with all transmitters excited, the cross-coupled power can be observed to reflect the S matrix description. FIG. 3 shows the vacuum characteristics of the antenna for $0\text{-}\pi\text{-}0\text{-}\pi\text{-}0\text{-}\pi$ phasing of the transmitters. The amplitude of the rf voltage and the phase at the feedpoints of the antenna circuit are shown, reflecting the desired phasing and the amplitude balance.

In the presence of plasma the antenna circuit is loaded down by the launching of wave energy into the plasma and has an added mutual inductance to reactive currents excited in the plasma. The antenna radiation resistance masks the effect of the antenna mutual inductance and, if sufficiently large, allows the various elements to operate independently of each other. The reactive part of the plasma loading changes the resonant frequency of the inner loops and, if large enough, can lead to asymmetries in the antenna currents. In plasma the triplet coupling of the feedlines is much reduced or absent; i.e. the real part of the plasma loading is large enough to essentially suppress the mutual coupling effect. The largest cross-coupled power is now observed on the line adjacent to the one excited in the co-toroidal direction. This

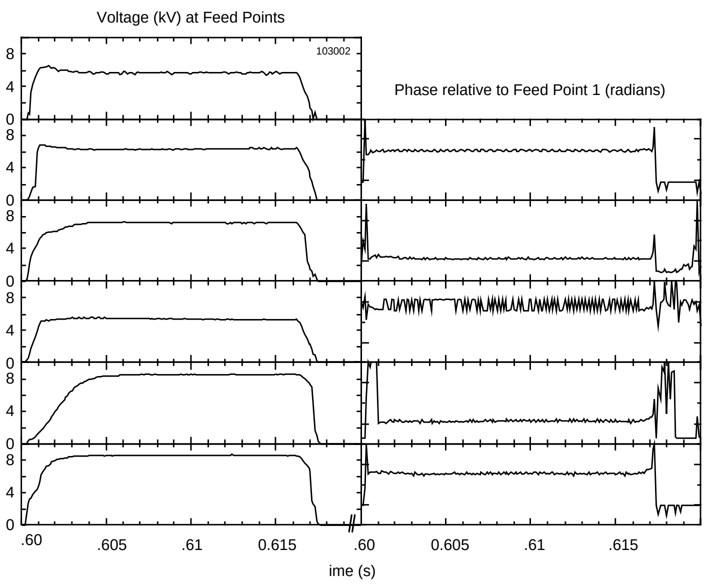

Figure 3 Antenna Voltage (kV), left, and phase (radians)

asymmetry in the cross-coupled power may indicate an asymmetry in the wave propagation in the toroidal direction. Coupling codes have predicted this asymmetry to be present due to the large pitch angle of the magnetic field at the plasma edge.

The observed properties of the coupling network are in agreement with the design expectations and allow satisfactory phase control with equal power from each of the six transmitters.

4. Heating Results

HHFW power has been applied to several NSTX target plasmas. Helium and deuterium plasmas with currents from 500 to 700 kA have been explored. Center stack limited and double null diverted configurations have been employed. FIG. 4 shows the time evolution of a 700 kA Helium plasma into which 2.3 MW of rf power is applied starting at 160 ms. The central electron temperature increases from 400 eV to 900 eV during the rf heating while the line density remains constant. The loop voltage falls to 1.0 V as compared to 1.35 V on an identical no rf shot. The total plasma stored energy reaches 53 kJ as opposed to 43 kJ. A maximum stored energy of 58 kJ with 2.9 MW of power was obtained. In FIGS. 5 and 6, density and temperature profiles from Thomson scattering are shown for the case of FIG. 4. The temperature increase is seen to be broad in radius and accompanied by little density increase. Confirmation of the temperature increase is seen with an x-ray crystal spectrometer which yields a central temperature of 1 keV. Plasma radiation as measured by bolometry shows a small increase in edge radiation, which is attributed to an increase in carbon. However, the total radiated power remains low at < 10%.

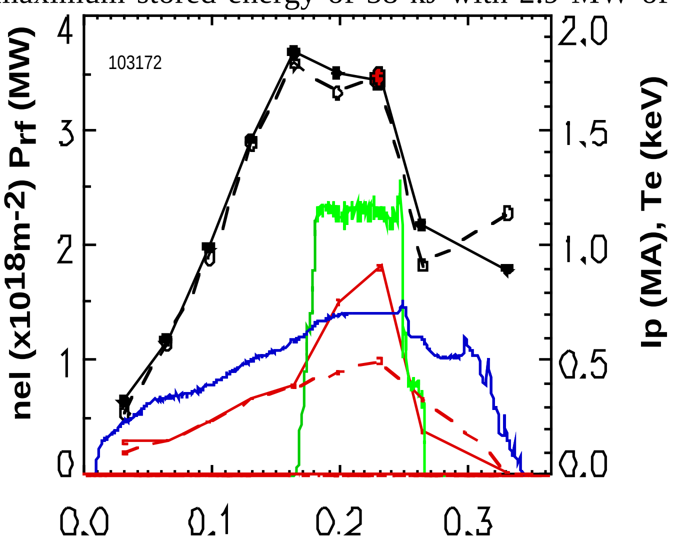

Figure 4 Time evolution of line density (black), plasma current (blue), Central electron temperature (red) and rf power (green)

In deuterium plasmas a larger density increase is observed. A stored energy of 43 kJ is measured for an rf power of 2 MW with the ohmic comparison showing 34 kJ. The lower stored energies obtained in deuterium are typical for NSTX. The temperature increase is smaller than in the helium case. A low target density deuterium plasma, $n_{el} = 4x10^{18}$ m^{-2}, has also been heated successfully. Radiated power profiles are similar to the helium case with a modest increase in edge radiation but total radiated power remaining small, <10%.

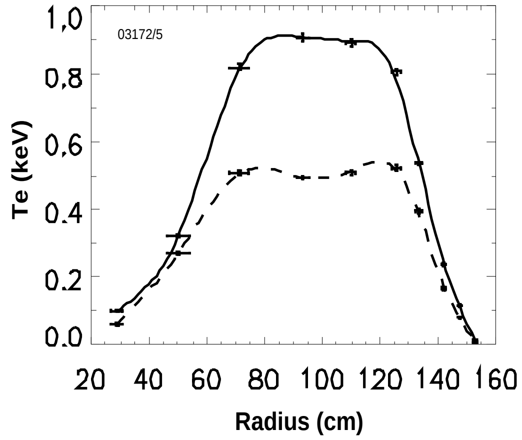

Figure 5 Electron temperature profiles at t=0.23 s, with (solid) and without (dashed) rf

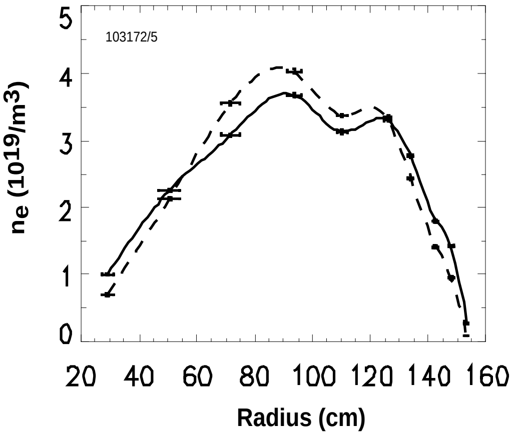

Figure 6 Electron density profiles for t=0.23 s, with (solid) and without (dashed) rf

MHD stability appears to be playing a role in limiting the plasma performance in both the rf heated and ohmic plasmas. An m=1, n=1 oscillation is present beginning with the plasma current flattop. This instability broadens the temperature and density profiles and subsequently the discharge parameters degrade with the occurrence of the first sawtooth. The sawtooth oscillation appears to allow plasma contact with a wall surface and sharply increases the carbon and hydrogen light. In the rf heated plasmas, the sawtooth occurs earlier and becomes larger as more rf power is applied. The sawtooth driven edge perturbation can be large enough at higher powers to trip off the rf transmitters due to high power reflection. This sawtoothing behavior often precedes a more violent MHD event, which can dump a significant fraction of the plasma out of the discharge.

5. Modeling of HHFW Discharges

Modeling of the power deposition of HHFW in an ST equilibrium is challenging because of the multiple high harmonic cyclotron resonances and the strong magnetic shear. Both 1D and 2D kinetic wave codes have been applied. Single pass absorption estimates are obtained with the 1D integral code, METS [5]. For the conditions of the shot shown in FIGS. 4, 5 and 6, METS predicts that the rf power should be absorbed on the electrons well off-axis in a single pass. For this calculation a toroidal wavenumber of 14 m^{-1}, corresponding to the peak in the antenna vacuum spectrum, was assumed.

Simulation results, from the 2D FLR kinetic wave code TORIC [6], are in good qualitative agreement with METS for this experiment. The 2D absorption profile is peaked well off-axis. When poloidal field effects on the wave propagation are included, an increase in wave penetration for the actual case is predicted which may correspond to some downshifting of the toroidal wave spectrum.

The use of helium plasmas was partially motivated by the prediction that ion damping at the helium cyclotron harmonics would be less than that at the corresponding deuterium cyclotron harmonics. This decrease is due to the smaller gyro radius for helium at the same temperature. This effect becomes important at ion temperatures above 1 keV. In addition helium plasmas generally contain much less hydrogen which can have stronger cyclotron damping since it is at a smaller harmonic number (eighth harmonic for the cases here).

6. Summary and Future Directions

Successful operation of the NSTX HHFW rf heating system has begun. A twelve-element antenna array powered by six transmitters has been used to inject up to 3.85 MW of rf power into NSTX. Strong electron heating has been observed as predicted by theory. Temperature increases from 400 to 900 eV have been observed in helium plasmas with a power of 2.3 MW. These increases are accompanied by little or no increase in the plasma density. Plasma and antenna performance degrades as a result of sawtooth oscillations and strong MHD events that eject plasma to the wall surfaces.

Variation of the antenna phasing to control the electron heating deposition profile as well as to drive plasma current are the next stage in HHFW experiments. Exploration of the role of ion damping into bulk ions, minority hydrogen ions or energetic neutral beam ions will play a crucial role as plasma temperatures are increased further.

7. References

[1] ONO, M., et al., Proceedings of the 18th IEEE/WPSS Symposium on Fusion Engineering, Alburqueque NM (1999), 53.

[2] ONO, M., Physics of Plasmas, **2**, (1995) 4075.

[3] SWAIN, D. W., et al., Proc. 27th EPS Conf. on Controlled Fusion and Plasma Physics, Budapest, Hungary, (2000).

[4] RYAN, P. M., et al., Proceedings of the 21st Symposium on Fusion Tech. Madrid Spain, (2000),

[5] SMITHE, D. N., “METS95: A High Temperature Plasma Wave Analysis Tool,” MRC/WDC-R-363, November 1995.

[6] BRAMBILLA, M., Plasma Physics and Controlled Fusion **41** (1999) 1.

The Princeton Plasma Physics Laboratory is operated
by Princeton University under contract
with the U.S. Department of Energy.

Information Services
Princeton Plasma Physics Laboratory
P.O. Box 451
Princeton, NJ 08543

Phone: 609-243-2750
Fax: 609-243-2751
e-mail: pppl_info@pppl.gov
Internet Address: http://www.pppl.gov